frontiers | Frontiers in Physics

TYPE Original Research
PUBLISHED 30 October 2024
DOI 10.3389/fphy.2024.1497190

OPEN ACCESS

EDITED BY
Huiming Tan,
Hohai University, China

REVIEWED BY
Yongfeng Deng,
Southeast University, China
Xingyue Li,
Tongji University, China

*CORRESPONDENCE
Peiqing Wang,
497450734@qq.com

RECEIVED 16 September 2024
ACCEPTED 16 October 2024
PUBLISHED 30 October 2024

CITATION
Sang D, Wang P, Chen L, Zhang W, Liu Z and Wang Q (2024) Analysis of the mechanical properties and micro-reinforcement mechanisms of loose accumulated sandy soil improved with polyvinyl alcohol and sisal fiber. *Front. Phys.* 12:1497190.
doi: 10.3389/fphy.2024.1497190

Analysis of the mechanical properties and micro-reinforcement mechanisms of loose accumulated sandy soil improved with polyvinyl alcohol and sisal fiber

Ding Sang[1,2], Peiqing Wang[1,2]*, Liang Chen[1,2], Wengang Zhang[3], Zhen Liu[1,2] and Qi Wang[1,2]

[1]College of Water Conservancy and Civil Engineering, Xizang Agriculture and Animal Husbandry University, Linzhi, China, [2]Research Center of Civil, Hydraulic and Power Engineering of Xizang, Xizang Agriculture and Animal Husbandry University, Linzhi, China, [3]School of Civil Engineering, Chongqing University, Chongqing, China

As one of the world's most fragile and sensitive ecological regions, Xizang risks significant environmental damage from using traditional materials, including cement and lime, to improve and reinforce loose accumulated sandy soil slopes. To address this issue, this study utilized a low-concentration biodegradable polyvinyl alcohol (PVA) solution combined with sisal fibers (SFs) to stabilize loose accumulated sand in southeastern Xizang. A series of physical, mechanical, and microscopic analyses was conducted to evaluate the properties of the treated sand. The results indicated the following. 1) The stress-strain curves of the improved samples exhibited an elastic-plastic relationship. Failure was observed in two stages. At a strain of 3% or less, the samples demonstrated elastic deformation with a linear increase in stress, whereas the deviator stress increased rapidly and linearly with an increase in axial strain. Once the strain exceeded 3%, the deformation became plastic with a nonlinear increase in the stress-strain relationship, and the growth rate of the deviator stress gradually decreased and leveled off. 2) Under varying confining pressure conditions, the relationship curve between the maximum $(\sigma_1\text{-}\sigma_3)_{max}$~$\sigma_3$ for both untreated loose accumulated sandy soil and soil improved with the PVA solution, and the sisal fiber was approximately linear. 3) The SFs created a skeletal-like network that encased the soil particles, and the hydroxyl functional groups in the PVA molecules bonded with both the soil particles and the fiber surface, thereby enhancing the interfacial properties. This interaction resulted in a tighter connection between the soil particles and SFs, which improved the stability of the structure. 4) The incorporation of a PVA solution and SFs significantly enhanced the mechanical strength and deformation resistance of the loose accumulated sandy soil. The optimal ratio for the improved soil was S_P = 3% and S_L = 15 mm, which increased the cohesion from 24.54 kPa in untreated loose accumulated sandy soil to 196.03 kPa. These findings could be applied in

engineering practices to improve and reinforce loose accumulated sandy soil slopes in southeastern Xizang and provide a theoretical basis for such applications.

KEYWORDS

southeastern xizang, loose accumulated sandy soil, polyvinyl alcohol, sisal fiber, triaxial test, mechanism analysis

1 Introduction

The southeastern region of Xizang is characterized by rugged mountains and intricate valleys, where diverse topographies and highland environments create a complex and unique climate that accelerates rock erosion and weathering. Over time, geological processes have transformed landscapes, resulting in extensive loose accumulation of sandy soil slopes after weathering. Sandy soil, as a typical non-cohesive soil, has a loose structure and low cohesion [1], making it prone to rainfall-induced erosion, which can lead to landslides and debris flows, posing significant threats to the lives and properties of local residents [2–10]. Therefore, research on the improvement and reinforcement of loose accumulated soil is crucial to mitigate landslides and debris flows triggered by rainfall.

As global ecological issues escalate, countries are advancing their environmental protection strategies. Scholars are exploring new high-polymer materials and natural fibers as alternatives to traditional soil reinforcement materials such as cement and lime [11–13]. Polymer-based reinforcement techniques are environmentally friendly, in which polymers facilitate chemical reactions that transform liquid substances into solid forms, thereby binding loose sandy soil into a more robust structure. Polyvinyl alcohol (PVA) is a polymer that enhances soil water stability by forming a gel-soil bonding system with soil particles, thus improving both strength and water stability [14–17]. Cherdsak et al. [18] demonstrated a significant increase in the unconfined compressive strength of soil with the addition of PVA, and Cruz et al. [19] developed a novel biopolymer hydrogel using PVA to enhance soil water retention. Owing to their degradability, renewability, cost-effectiveness, and strong mechanical properties [13, 20–22], natural fibers are a major focus of geotechnical engineering. Various natural fibers, including palm, sisal, bamboo, and areca, have been employed for soil improvement with satisfactory reinforcement results [13, 23, 24]. Sisal fiber (SF) known for its toughness, strength, and resistance to wear and corrosion under harsh conditions is increasingly being applied as a reinforcement material for both inorganic and organic binding agents [25]. The high-strength characteristics of sisal fibers are closely related to their chemical composition and structure. They mainly contain components, such as cellulose, hemicellulose, pectin, and lignin, which together constitute a robust framework for fibers. Cellulose, as the primary structural component, endows sisal fibers with high strength and elasticity, and hemicellulose, pectin, and lignin further enhance their wear and corrosion resistance [26]. For instance, Sharanabasava Patil et al. [27] adopted SFs to enhance coarse aggregates in fly ash-red soil concrete, promoting sustainable concrete development. Song H et al. [28] employed the SFs to reinforce the synthesized aggregates. Aimin Z et al. [29] replaced the traditional steel fibers with mixed SFs to create UHPC materials, utilizing long (12 mm) and short (6 mm) fibers (2% fiber content). Additionally, Ekkachai Y et al. [30] demonstrated that SFs improved the structural performance of reinforced concrete columns, and Lima R P et al. [31] evaluated their effectiveness in enhancing the bending strength of one-way precast concrete slabs after cracking.

The aforementioned studies suggest that both PVA and SFs are eco-friendly materials for soil improvement. However, little research has focused on the mechanisms by which soil, fibers, and polymers interact to enhance loose accumulated sandy soils. This study addressed this gap by employing varying concentrations of PVA solutions and different lengths of SFs to improve sandy soil, quantitatively analyzing their effects on the mechanical properties of the improved soil, and investigating the intrinsic microstructural changes in the reinforced soil. These findings provide a theoretical basis and practical guidance for protecting and reinforcing loose accumulated sandy soil slopes in southeastern Xizang.

2 Experimental overview

2.1 Experimental materials

The sandy soil adopted in this experiment was sourced from loose accumulated sandy soil slopes along National Highway 318 in Bomi County, southeastern Xizang (Latitude 30°16′78″, Longitude 94°94′35″), at a sampling depth of approximately 2 m. After the soil

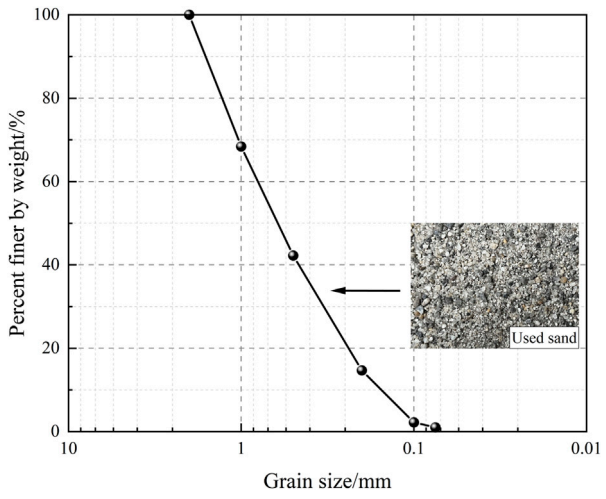

FIGURE 1
Grain size distribution curve of test sandy soil.

TABLE 1 Main physical and mechanical properties of sandy soils.

$\rho_{d\,max}$/ (g.cm^{-3})	ρ_d/ (g.cm^{-3})	$\rho_{d\,min}$/ (g.cm^{-3})	ω/ %	D_{50}/ mm	C_u	C_c
2.13	1.93	1.72	1.15	0.614	2.4	0.9

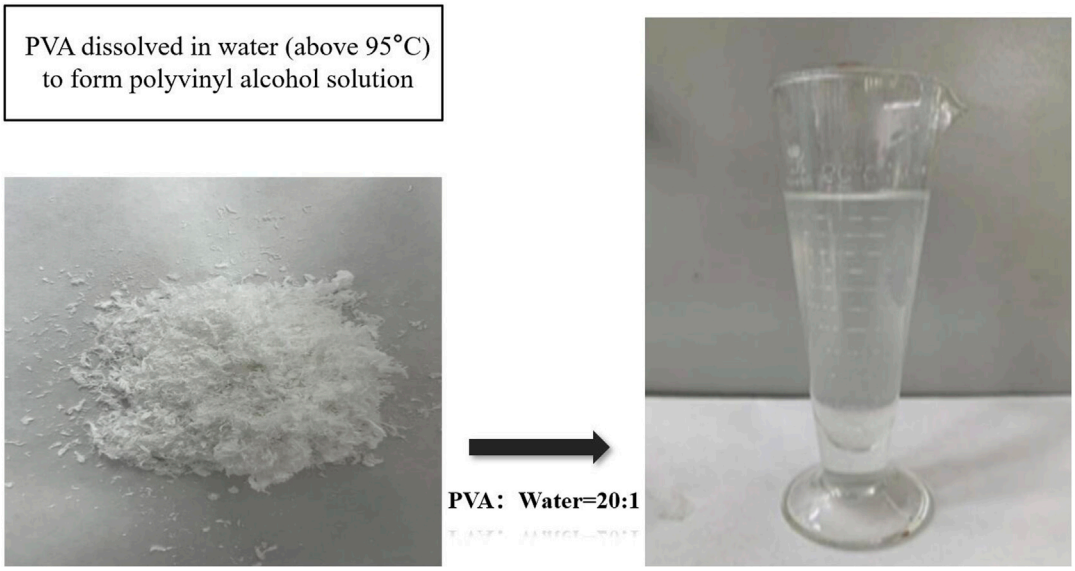

FIGURE 2
Polyvinyl alcohol solution.

TABLE 2 Basic physical properties of polyvinyl alcohol.

Viscosity/ mPa.s	Volatile matter/%	Ash content/%	pH
34.0-42.2	5	0.5	5.0-7.0

samples were retrieved, they were dried in an oven and subjected to sieve analysis according to the "Standard for Geotechnical Testing Methods" (GB/T 50123-2019) [32], resulting in the cumulative particle size distribution curve shown in Figure 1. Additional basic physical properties of the sandy soil are listed in Table 1.

The polymer utilized in this experiment was PVA (Figure 2). It is a polyhydroxy polymer valued for its water solubility, barrier properties, and biodegradability, and has the chemical formula $[C_2H_4O]_n$. It appears as a white, flaky, fibrous, or powdered solid that is odorless and soluble in water at temperatures above 95°C. In the experiment, the PVA solution was prepared by dissolving PVA in boiling water at a specific ratio. PVA has a lower degree of hydrolysis and retains some hydroxyl groups, enhancing its cohesive properties. The reaction process is shown in Equation 1, and the physical parameters are summarized in Table 2.

$$(C_2H_4O)_n + nH_2O \rightarrow nC_2H_50H + OH^- \quad (1)$$

where $(C_2H_4O)_n$ represents PVA; H_2O represents water molecules; C_2H_5OH signifies the ethanol; and OH^- denotes the hydroxide ions.

The SFs used in this experiment were natural bundled fibers, widely recognized for their advantages, such as low energy consumption, low manufacturing costs, high elasticity, large elastic modulus, acid and base resistance, and rapid water absorption. Considered ideal reinforcement materials for both inorganic and organic binders, their strength increased by 10%–15% in water compared to their dry strength [33]. These fibers were environmentally friendly with a rough surface texture, good dispersion, an average diameter of approximately 0.2 mm, and biodegradability. For the experiment, SFs with lengths of 6 mm, 9 mm, 12 mm, and 15 mm were selected (Figure 3). This study examined the effect of SFs length (S_L) on the mechanical properties of reinforced sandy soil, with the SFs content (S_F) defined as the ratio of the mass of SFs (m_d) to the mass of dry sand (m_s), calculated using the following Equation 2.

$$S_F = \frac{m_d}{m_s} \quad (2)$$

2.2 Experimental instruments

The triaxial shear test was performed using a 6T-type fully automatic triaxial shear apparatus consisting of three main components: a pressure chamber, a pressure volume controller, and a data processing system. The sample parameters were initialized using software, and various sensors automatically collected the data via a data processing system. The equipment used is illustrated in Figure 4. To analyze the microstructural changes in the loose accumulated sandy soil reinforced with SFs and PVA solution, a CX-200PLUS tungsten filament scanning electron microscope (SEM) was employed on the shear-tested samples. This SEM included an electron gun, a sample stage, electron lenses, detectors, an electron scanning system, a control system, a display, and image processing software (Figure 5).

2.3 Experimental procedure

Before the experiment, sandy soil was prepared according to the cumulative curve of the particle size distribution. To ensure a

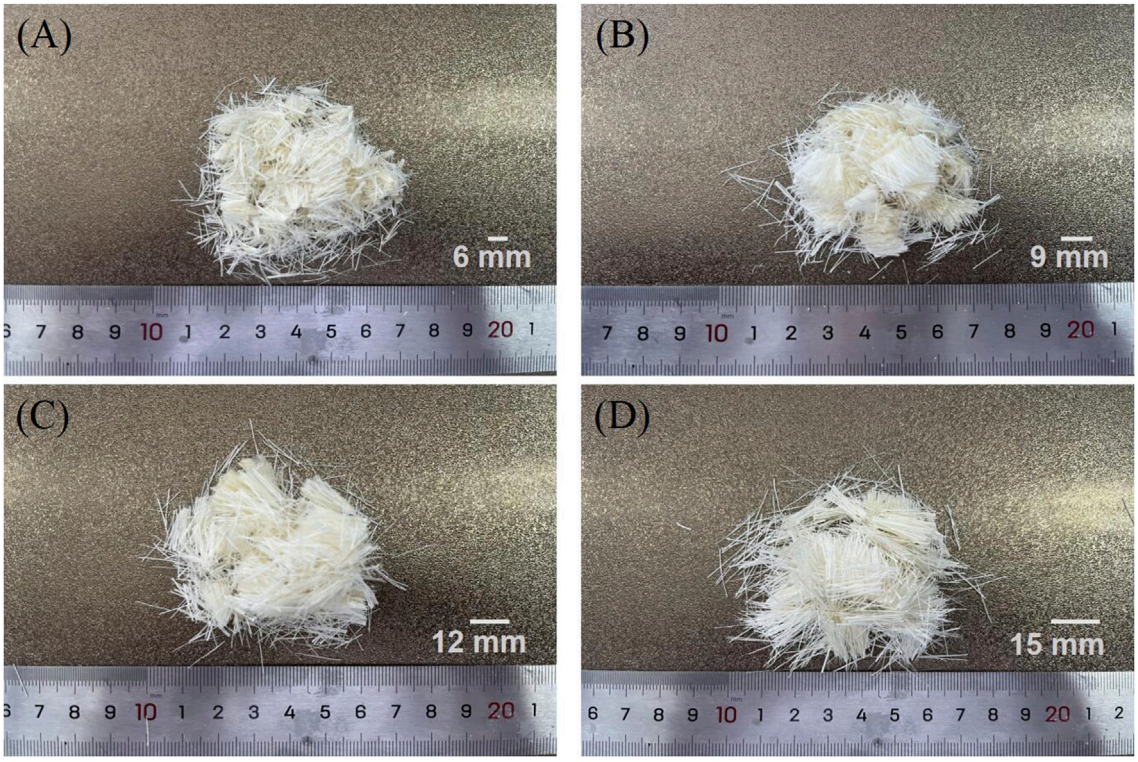

FIGURE 3
Sisal fiber. **(A)** S_L = 6 mm, **(B)** S_L = 9 mm, **(C)** S_L = 12 mm, **(D)** S_L = 15 mm.

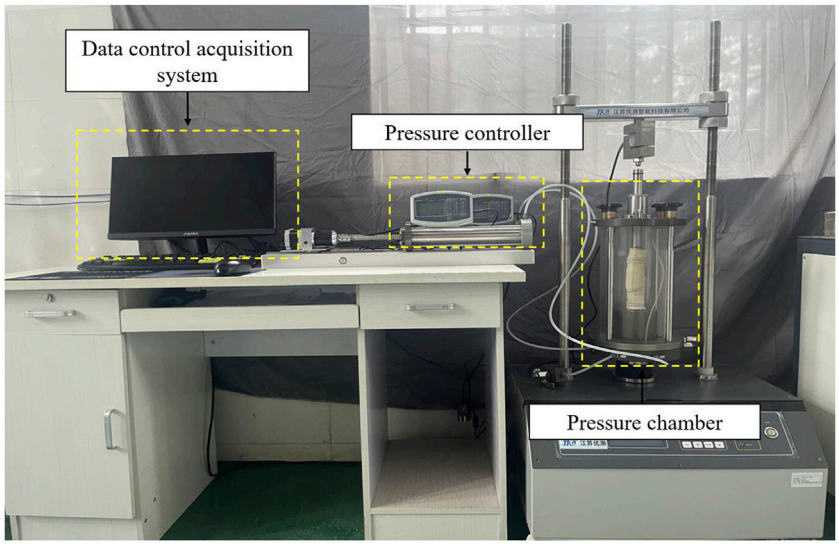

FIGURE 4
Fully automatic triaxial shear apparatus.

uniform distribution of SFs within the sandy soil, dry sand was thoroughly mixed with the fibers, followed by the addition of water and PVA solution to the mixture. The obtained soil-fiber mixture was compacted into a cylindrical mold in four layers, with each layer scarified using a soil cutter. The final cylindrical samples measured φ39.1 mm × h 80 mm. Triaxial shear tests were conducted using a 6T fully automatic triaxial apparatus, whereas microstructural analysis was performed using a CX-200PLUS tungsten filament scanning electron microscope (SEM). Each sample with identical parameters underwent three independent trials, and the most statistically

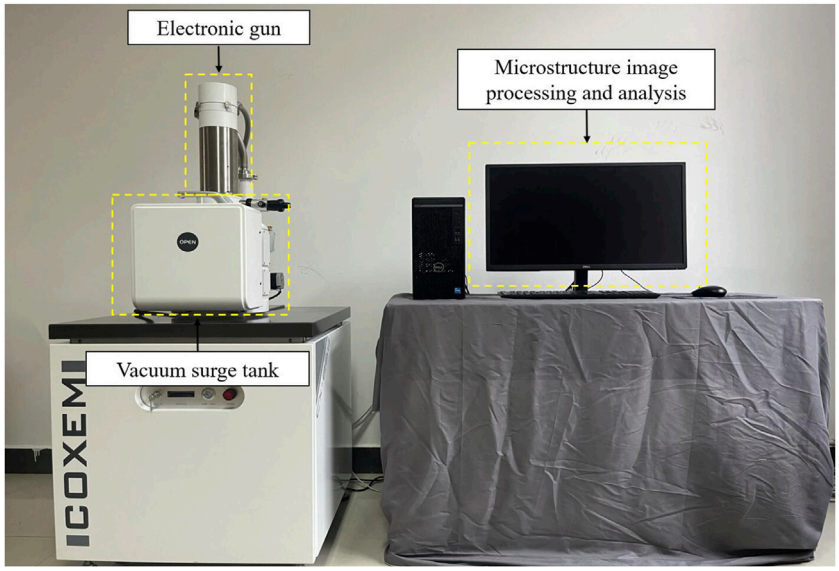

FIGURE 5
SEM scanning electron microscope.

significant data were selected for analysis. The detailed experimental procedure is as follows.

2.3.1 Triaxial shear test

A total of 25 groups of samples were prepared for this study, consisting of one group of untreated loose accumulated sandy soil and four groups of PVA-treated loose accumulated sandy soil.

The study prepared 4 groups of SFs-treated loose accumulated sandy soil and 16 groups of PVA and SF-reinforced loose accumulated sandy soil. Each group underwent consolidation drained shear testing under confining pressures of 100 kPa, 200 kPa, 300 kPa, and 400 kPa, following the "Standard for Geotechnical Testing Methods" (GB/T 50123—2019). The shear strain rate was set at 0.08 mm/min, and the testing was stopped when the strain (ε) reached 15%. To evaluate the effects of the PVA solution content (S_P) and SFs length (S_L) on the strength of the reinforced sandy soil, PVA solution contents of 1%, 2%, 3%, and 4% and SFs lengths of 6 mm, 9 mm, 12 mm, and 15 mm were tested, while the SFs content (S_F) remained constant at 0.8% (both PVA and fiber contents were percentages of the total sample mass). The initial moisture content was controlled at w = 1.15% and the density at ρ_d = 1.93 g/cm^3, with the untreated sandy soil of the same moisture content and density serving as a control.

2.3.2 Microstructural analysis

To prepare the samples for SEM observation, they were air-dried to remove moisture, volatile substances, and magnetic materials. After drying, internal samples of dimensions 10 mm × 5 mm × 2 mm were extracted for analysis. Because the sandy materials were non-conductive, directly placing them under the electron microscope could cause damage to the electron beam and reduce the edge resolution. To obtain high-quality images, the surfaces of the samples were coated with a metallic layer to minimize electron beam penetration and enhance the edge resolution, thus protecting the sensitive samples. CX-200PLUS SEM was then applied to observe the microstructural characteristics of the loose accumulated sandy soil before and after reinforcement with PVA solution and SFs, with a particular focus on the reinforcement mechanism.

3 Test results and analysis

3.1 Characteristics of deviator stress and axial strain curves

The deviator stress-strain curves for untreated loose accumulated sandy soil and sandy soil reinforced with PVA solution and SFs were plotted based on the results of triaxial consolidated drained shear tests (CD) (Figure 6).

In Figure 6A, the deviator stress-strain curve for the untreated loose accumulated sandy soil demonstrated that under varying confining pressures, the samples primarily exhibited strain softening. Initially, the samples exhibited elastic deformation with a linear increase in the strain. Once the strain exceeded 2%, the curve entered a nonlinear phase, where the rate of increase in the deviator stress gradually decreased, and higher confining pressures required greater axial strain to achieve the peak deviator stress. Figures 6B, C present the deviator stress-strain curves for sandy soil reinforced with a PVA solution, where the samples also demonstrated strain softening. At confining pressures of 100 and 200 kPa, the peak deviator stress fluctuated with increasing PVA solution content. In contrast, at 300 and 400 kPa, it gradually increased with increasing PVA content, whereas the peak values did not exhibit a significant improvement compared with the untreated sandy soil. The post-peak softening phenomenon improved, although the extent of this improvement was relatively modest. Figures 6D,E illustrate the

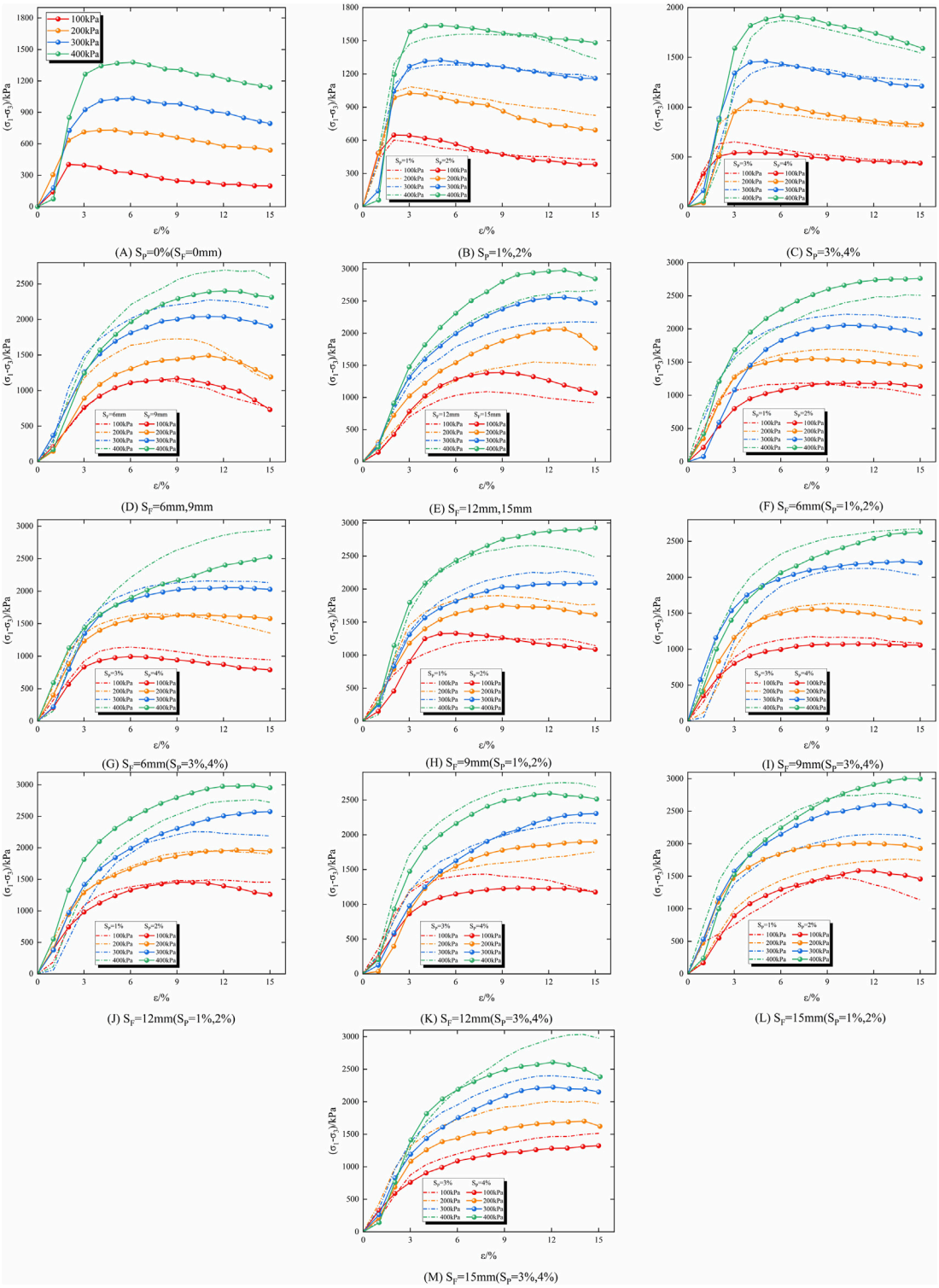

FIGURE 6
Deviator stress-strain curves of untreated loose accumulated sandy soil and modified loose accumulated sandy soil with PVA and SFs. Note: S_F is the length of sisal fiber, and S_P is the content of polyvinyl alcohol. **(A)** Untreated loose accumulated soil. **(B)** Modified loose accumulated sandy soil with PAV solution content of 1% and 2%. **(C)** Modified loose accumulated sandy soil with PAV solution content of 3% and 4%. **(D)** Modified loose accumulated sandy soil with SFs lengths of 6 mm and 9 mm. **(E)** Modified loose accumulated sandy soil with SFs lengths of 12 mm and 15 mm. **(F)** Modified loose accumulated sandy soil with SFs length of 6 mm and PAV solution content of 1% and 2%. **(G)** Modified loose accumulated sandy soil with SFs length of 6mm and PAV solution content of 3% and 4%. **(H)** Modified loose accumulated sandy soil with SFs length of 9mm and PAV solution content of 1% and 2%. **(I)** Modified loose accumulated sandy soil with SFs length of 9 mm and PAV solution content of 3% and 4%. **(J)** modified loose accumulated sandy soil with SFs length of 12 mm and PAV solution content of 1% and 2%. **(K)** modified loose accumulated sandy soil with SFs length of 12 mm and PAV solution content of 3% and 4%. **(L)** Modified loose accumulated sandy soil with SFs length of 15 mm and PAV solution content of 1% and 2%. **(M)** Modified loose accumulated sandy soil with SFs length of 15 mm and PAV solution content of 3% and 4%View less.

10.3389/fphy.2024.1497190

TABLE 3 Peak deviator stress of untreated loose accumulated soil and modified loose accumulated sandy soil with PVA solution and SFs.

Number	S_P/%	S_L/mm	S_F/%	Confining pressure/kPa			
				100	200	300	400
S-1	—	—	—	424	744	1,042	1,390
S-2	1	—	—	612	1,104	1,301	1,580
S-3	2	—	—	663	1,049	1,337	1,665
S-4	3	—	—	667	1,065	1,435	1887
S-5	4	—	—	558	1,081	1,472	1927
S-6	—	6	—	1,164	1749	2,296	2,729
S-7	—	9	—	1,184	1,496	2080	2,428
S-8	—	12	—	1,199	1873	2,188	2,685
S-9	—	15	—	1,405	2095	2,575	3,015
S-10	1	6	0.8	1,197	1716	2,231	2,538
S-11	2	6	0.8	1,197	1,565	2070	2,788
S-12	3	6	0.8	1,149	1,670	2,177	2,959
S-13	4	6	0.8	1,009	1,651	2076	2,750
S-14	1	9	0.8	1,266	1911	2,287	2,674
S-15	2	9	0.8	1,344	1755	2,107	2,928
S-16	3	9	0.8	1,192	1,650	2,142	2,691
S-17	4	9	0.8	1,088	1,577	2,233	2,646
S-18	1	12	0.8	1,510	1968	2,279	2,783
S-19	2	12	0.8	1,473	1976	2,594	3,002
S-20	3	12	0.8	1,410	1783	2,193	2,785
S-21	4	12	0.8	1,245	1919	2,323	2,610
S-22	1	15	0.8	1,497	1878	2,224	2,810
S-23	2	15	0.8	1,601	2023	2,721	3,020
S-24	3	15	0.8	1,517	2,116	2,418	3,056
S-25	4	15	0.8	1,353	1811	2,244	2,625

deviator stress-strain curves for the sandy soil reinforced with SFs, increasing the peak deviator stress compared with the untreated sandy soil. However, once the peak strength was reached, the deviator stress decreased sharply. Figures 6F–M depict the deviator stress-strain curves for the sandy soil reinforced with a combination of PVA solution and SFs, revealing an elastic-plastic stress-strain relationship. The failure of these samples occurred in two phases. For strains less than or equal to 3%, the samples exhibited elastic deformation with a linear increase in the deviator stress, whereas beyond 3% strain, they underwent plastic deformation. In this phase, the stress-strain relationship exhibited a nonlinear upward trend with a gradual decrease in the rate of increase in deviator stress, resulting in a plateau. The curves exhibited a clear inflection point and maintained a softening characteristic, indicating a distinct peak in the deviator stress, followed by only slight reductions post-peak.

3.2 Relationship between peak deviator stress and confining pressure

According to the "Standard for Geotechnical Testing Methods" (GB/T 50123—2019), the peak strength was recorded at the moment of peak during the shear process of the sample. If no peak strength was evident, the strength corresponding to ε = 15% was used as the peak strength. Table 3 presents the peak deviator stress for the untreated loose accumulated sandy soil and sandy soil reinforced with the PVA solution and SFs under various confining pressures. The table indicates that the peak deviator stress for the sandy soil reinforced with the combination of PVA solution and SFs increased monotonically with the PVA content and length of the SFs. For the PVA contents of S_P = 2% and S_P = 3% and the SF length of S_L = 15 mm, the peak deviator stresses reached 1,601 kPa, 2023 kPa, 2,721 kPa, and 3,020 kPa under different confining pressures. For S_L = 15 mm, the corresponding values were 1,517 kPa, 2,116 kPa, 2,418 kPa, and 3,056 kPa. Compared with the peak deviator stress of the untreated sandy soil (424 kPa, 744 kPa, 1,042 kPa, and 1,390 kPa), these values represented increases of 377%, 271%, 261%, and 217%, and 357%, 284%, 232%, and 219%, respectively. As the confining pressure increased, the peak deviator stress of the samples also increased, whereas the relative increase compared to the untreated sandy soil showed a declining trend.

The data in Table 3 were plotted in the $(\sigma_1 - \sigma_3)_{max} \sim \sigma_3$ relationship graph. Figure 7 demonstrates that the $(\sigma_1 - \sigma_3)_{max} \sim \sigma_3$ relationship curves for both the untreated sandy soil and the sandy soil reinforced with PVA solution and SFs exhibited a nearly linear relationship, influenced by the soil particle arrangement and aggregation. The fluctuating characteristics of the slope and intercept of the regression equation for the peak deviator stress can be analyzed using linear regression principles based on the least-squares method. The coefficient R^2 indicated the correlation between the fitted line and the experimental points, with a value closer to 1 representing a higher degree of fit. Figure 7 reveals that all the fitted lines had determination coefficients R^2 higher than 0.958, indicating a high degree of fit that could be used to predict the trends in the peak deviator stress for the untreated loose accumulated sandy soil and the variations in the PVA solution content and SF length under different confining pressures. To represent the relationship between the peak deviator stress changes influenced by both factors simultaneously, a simple linear model was employed, as described by the following Equation 3.

$$(\sigma_1 - \sigma_3)_{max} = a\sigma_3 + b \tag{3}$$

where a and b are the parameters associated with the characteristics of untreated loose accumulated sandy soil and sandy soil reinforced with PVA solution and SFs, respectively.

The relationship between parameters a and b with respect to the concentration of the PVA solution is illustrated using samples with varying concentrations of PVA solution and a SFs length of S_L = 15 mm (Figure 8). The results is shown in Equations 3, 4.

$$a = 0.1804x + 4.056 \tag{4}$$

$$b = 135.2x + 610.6 \tag{5}$$

where x is the PVA solution content (%).

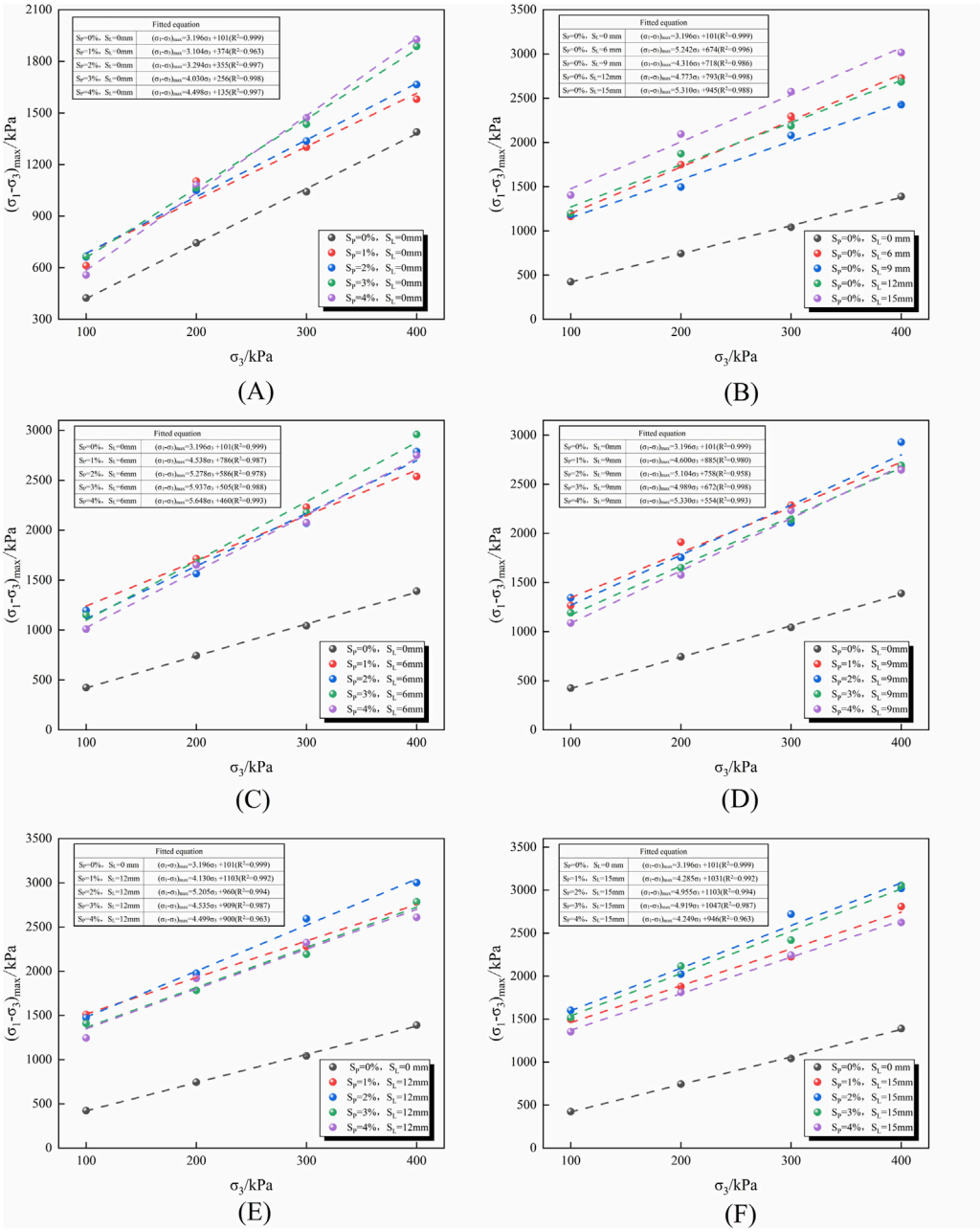

FIGURE 7
$(\sigma_1-\sigma_3)_{max}-\sigma_3$ relationship curve of untreated loose accumulated soil and modified loose accumulated sandy soil with PVA and SFs. **(A)** $(\sigma_1-\sigma_3)_{max}-\sigma_3$ relationship curve of untreated loose accumulated soil and modified loose accumulated sandy soil with different PVA solution contents **(B)** $(\sigma_1-\sigma_3)_{max}-\sigma_3$ relationship curve of untreated loose accumulated soil and modified loose accumulated sandy soil with different lengths of SFs **(C)** $(\sigma_1-\sigma_3)_{max}-\sigma_3$ relationship curve of untreated loose accumulated soil and modified loose accumulated sandy soil with S_L=6mm and different PVA solution contents **(D)** $(\sigma_1-\sigma_3)_{max}-\sigma_3$ relationship curve of untreated loose accumulated soil and modified loose accumulated sandy soil with S_L=9mm and different PVA solution contents **(E)** $(\sigma_1-\sigma_3)_{max}-\sigma_3$ relationship curve of untreated loose accumulated soil and modified loose accumulated sandy soil with S_L=12mm and different PVA solution contents **(F)** $(\sigma_1-\sigma_3)_{max}-\sigma_3$ relationship curve of untreated loose accumulated soil and modified loose accumulated sandy soil with S_L=15mm and different PVA solution contents.

3.3 Shear strength characteristics

Shear strength is a crucial index in geotechnics, represented by shear strength parameters. To elucidate the influence of the PVA solution content and SFs length on these parameters, the cohesion (c) and internal friction angle (φ) values were calculated for both untreated loose accumulated sandy soil and sandy soil reinforced with PVA solution and SFs.

Figure 9 presents a bar chart illustrating the relationship between the shear strength parameters and varying PVA solution content, including the parameters for the untreated loose accumulated sandy soil for comparison. As shown in Figure 9A, incorporating the PVA

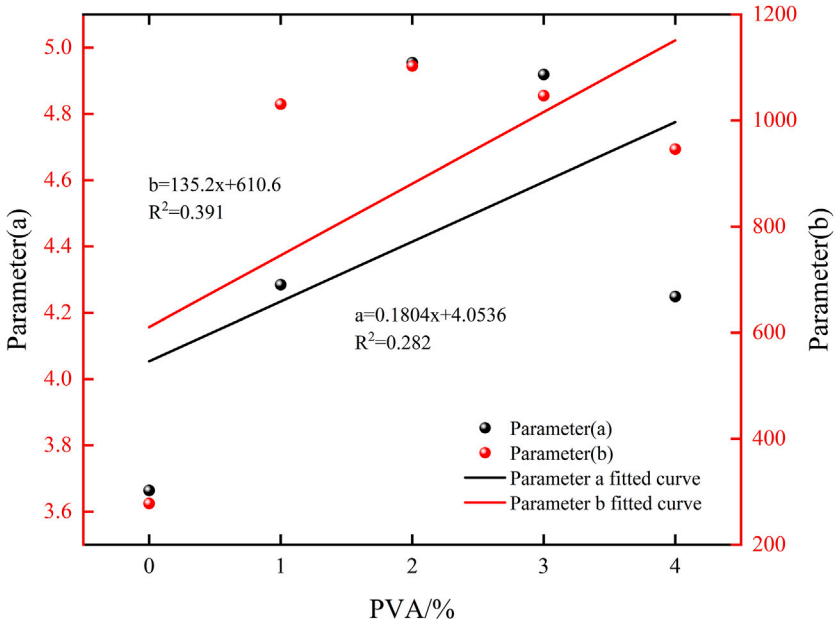

FIGURE 8
Curve fitting for the effect of peak bias stress with different PVA content at S_L = 15 mm.

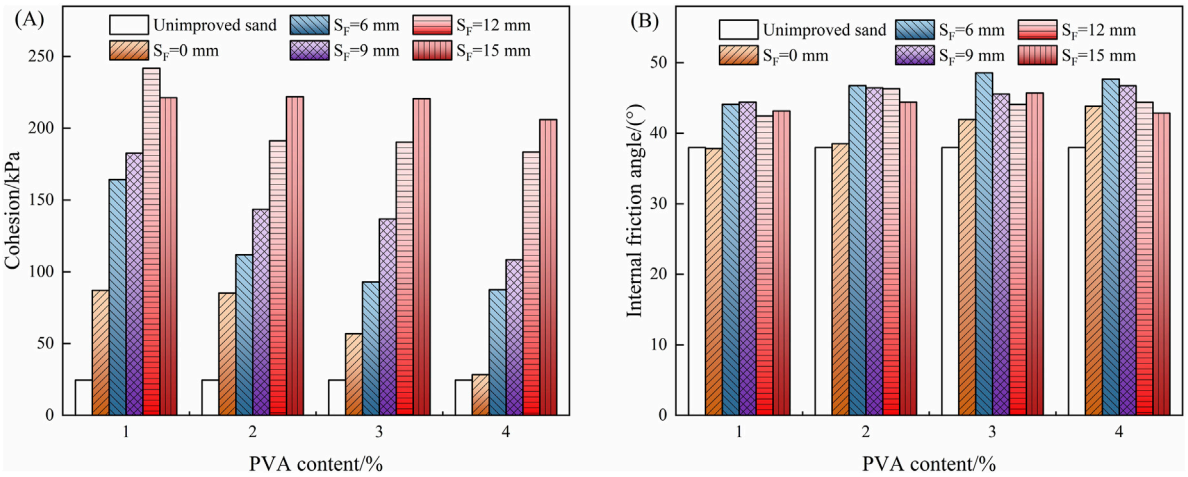

FIGURE 9
Relationship between shear strength parameters and PVA content. **(A)** relationship between cohesion and PVA content, **(B)** relationship between internal friction angle and PVA content.

solution significantly enhanced the cohesion of the samples compared with that of the untreated sandy soil. However, as the PVA content increased, the cohesion decreased. This trend suggested that while excess PVA effectively coated and intertwined the sandy particles, its wet and slippery characteristics during shear caused sliding among the PVA-coated particles, weakening their interconnections and reducing their cohesion. Conversely, Figure 9B illustrates that for the samples compounded with both the PVA solution and SFs, the internal friction angle initially increased with the PVA content but then decreased. The fluctuations in this parameter were relatively small, indicating that the significant changes observed in the cohesion were not reflected in the internal friction angle.

Figure 10 presents a bar chart illustrating the relationship between the shear strength parameters and varying SFs lengths, with untreated sandy soil parameters for comparison. Figure 10A reveals that with a constant PVA solution content, the cohesion of the reinforced sandy soil increased as the length of the SFs increased, peaking at 241.76 kPa for S_L = 12 mm (S_P = 1%). However, as the SFs length continued to increase, the cohesion decreased, with S_L = 15 mm (S_P = 1%) showing a cohesion value of 221.34 kPa. These values represented 985% and 901% of the cohesion of untreated sandy soil (24.54 kPa). The cohesion trend for the S_L = 12 mm sample exhibited a rapid initial increase that gradually stabilized, in contrast to the trend for the S_L = 15 mm sample.

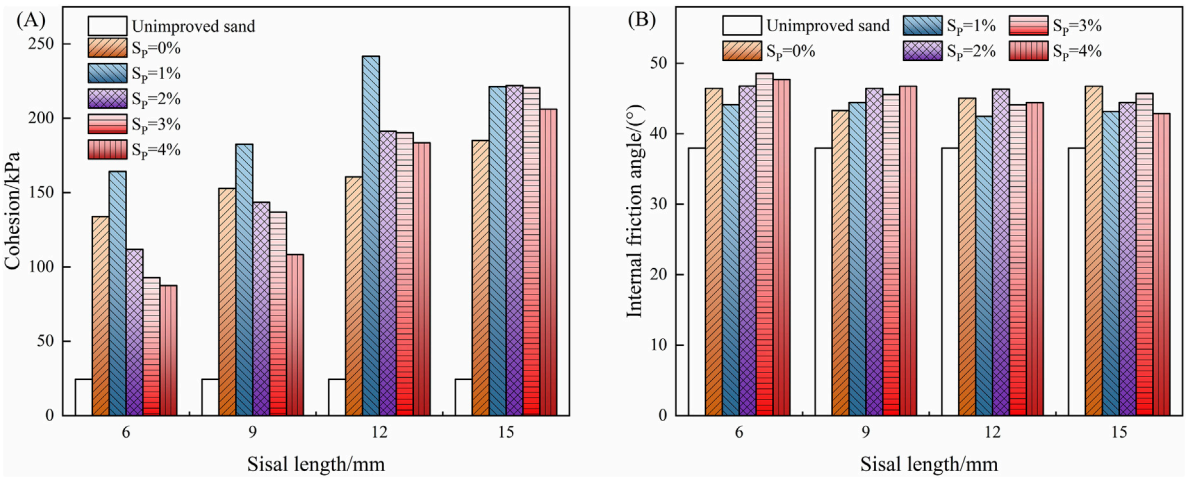

FIGURE 10
Relationship between shear strength parameters and SFs lengths. **(A)** relationship between cohesion and SFs length, **(B)** relationship between internal friction angle and SFs length.

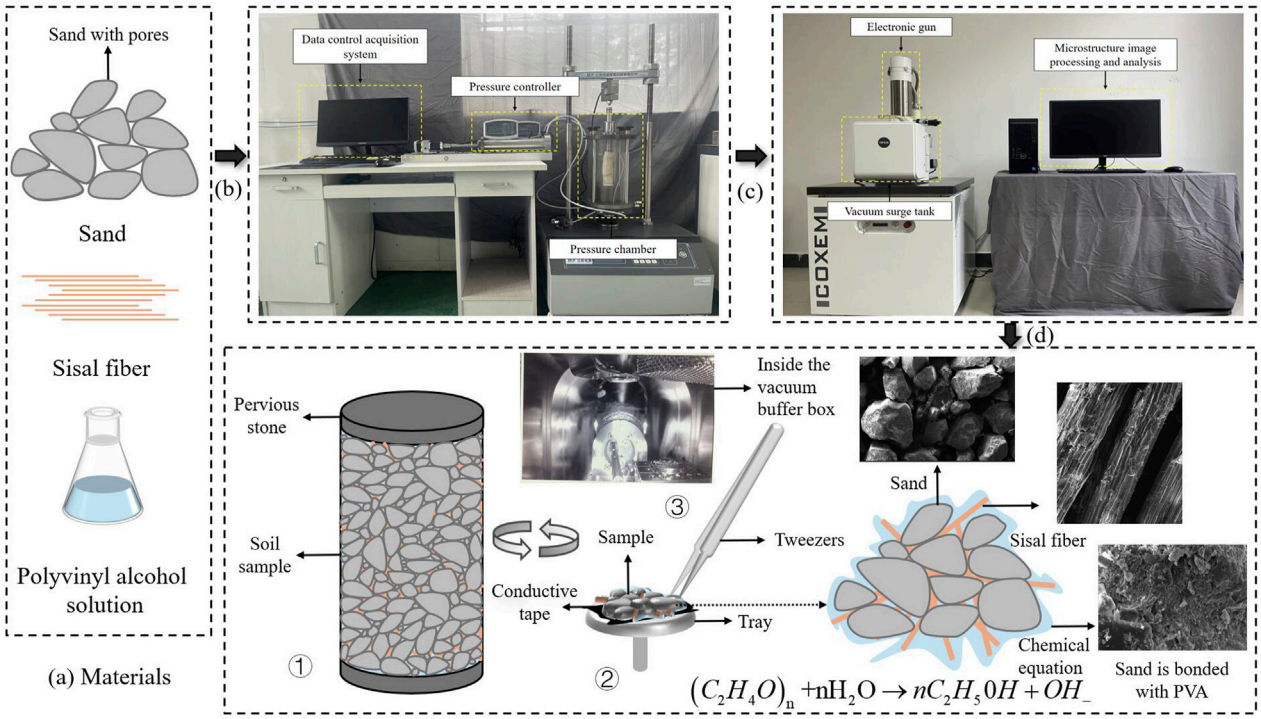

FIGURE 11
Schematic diagram of the mechanism of reinforcing sandy soil with PVA and SFs composite. **(A)** Experimental materials. **(B)** Triaxial test. **(C)** SEM experiment. **(D)** Microscopic analysis.

Figure 10B shows that the internal friction angle of the reinforced sandy soil exhibited a waveform pattern as the SFs length increased with minimal overall fluctuation. The changes in the internal friction angles were all less than 4°. This indicated that the PVA solution improved the bonding between the SFs and soil particles, thereby reducing the particle spacing. During shear, this enhanced the interlocking and friction intensity among the soil particles, leading to variations in the internal friction angle.

4 Mechanism analysis and discussion

4.1 Microscopic mechanism analysis

The mechanism of reinforcing loose accumulated sandy soil using a composite of PVA solution and SFs is illustrated in the schematic diagram in Figure 11. To analyze the microscopic structural characteristics of untreated loose accumulated sandy

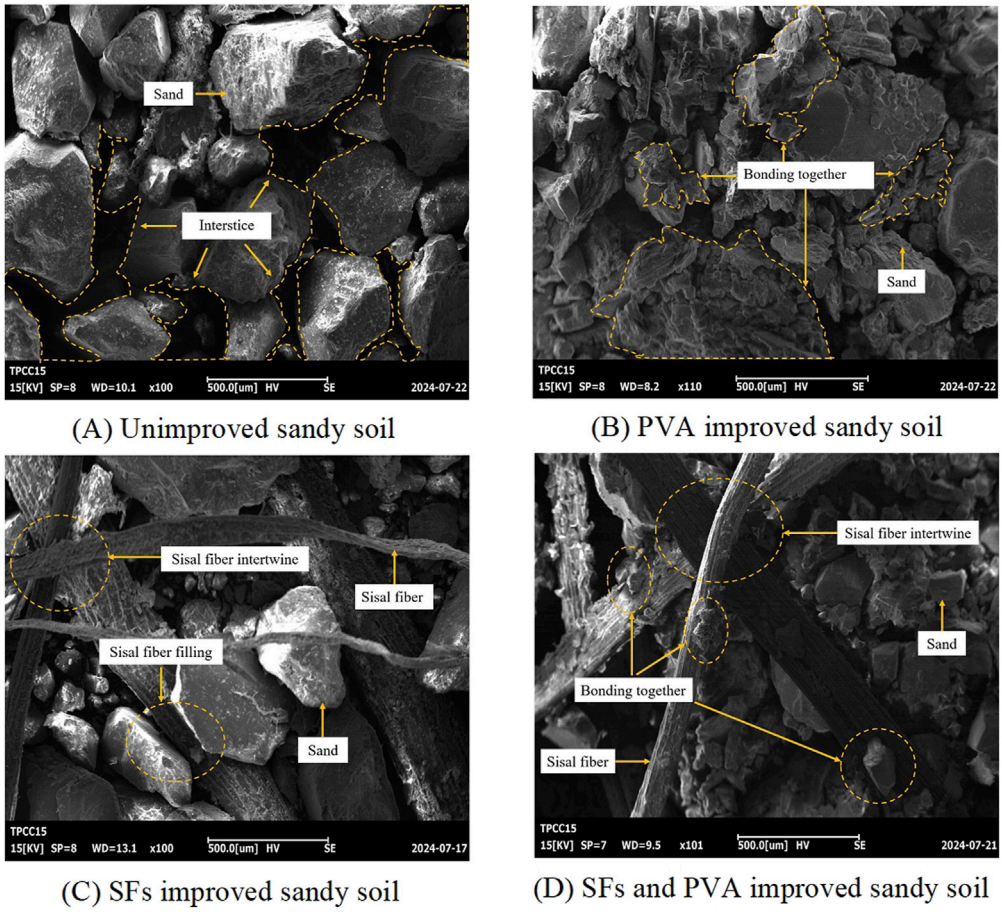

FIGURE 12
SEM images of untreated loose accumulated soil and modified loose accumulated sandy soil with PVA solution and SFs. **(A)** Unimproved sandy soil **(B)** PVA improved sandy soil **(C)** SFs improved sandy soil **(D)** SFs and PVA improved sandy soil.

soil, PVA solution, and SF-reinforced sandy soil, SEM with a tungsten filament (CX-200PLUS) was used (Figure 12). Sandy soil primarily consisted of sand grains that were non-cohesive and relied on particle interlocking and friction for stability. Figure 12A shows that the untreated loose accumulated sandy soil had a loose structure with a wide distribution of pore spaces between the particles. The cohesive PVA solution wrapped around and intertwined the sandy particles, improving their arrangement and facilitating more compact packing, thereby reducing the pore spaces. Figure 12B demonstrates how the PVA solution formed a solidified membrane around the sand grains, tightly bonding them to create a "granular structure" with enhanced strength and shape stability. Loose accumulated sandy soil, characterized by rough, angular particle surfaces, consists of debris that remained in its original position after weathering, leading to certain voids between bonded sand grains. As an ideal reinforcing material with both inorganic and organic binding properties, SFs were randomly distributed among the sandy particles, forming a woven "net" that enveloped the soil and reduced displacement and deformation. Figure 12C presents the SFs filling the spaces between the soil particles intersecting to form a fibrous network binding the grains together. These fibers distributed within the pores restricted radial deformation and enhanced the overall stability of the soil structure. The cohesion provided by the PVA solution synergized with the SFs anchoring effect, resulting in a stable structure that significantly improved the mechanical properties of the loose accumulated sandy soil.

Figure 12D shows that the soil particles were interconnected through the bonds among themselves, between the soil particles and fibers, and among the fibers. The voids between the sand grains were filled with SFs and the PVA solution. The intertwined SFs were effectively anchored within the adhesive formed by the PVA solution, enhancing the particle cohesion. The exceptional toughness of the SFs allowed them to connect across the fractures like "spider silk," providing the tensile strength and preventing the deformation of the sandy soil. The PVA solution exhibited strong adhesion to the fiber-containing materials, with hydroxyl functional groups bonding with the surfaces of both the soil particles and fibers, improving the interfacial properties and creating a tighter connection. This enhanced bonding significantly increased the stability of the composite structure formed by the SFs and sandy soil. The incorporation of the PVA solution and SFs formed a stable composite structure, improving the overall stability and safety of the soil matrix. The synergistic effect of the PVA solution and SFs enhanced the mechanical properties of the soil and contributed to its resilience to deformation and failure under load.

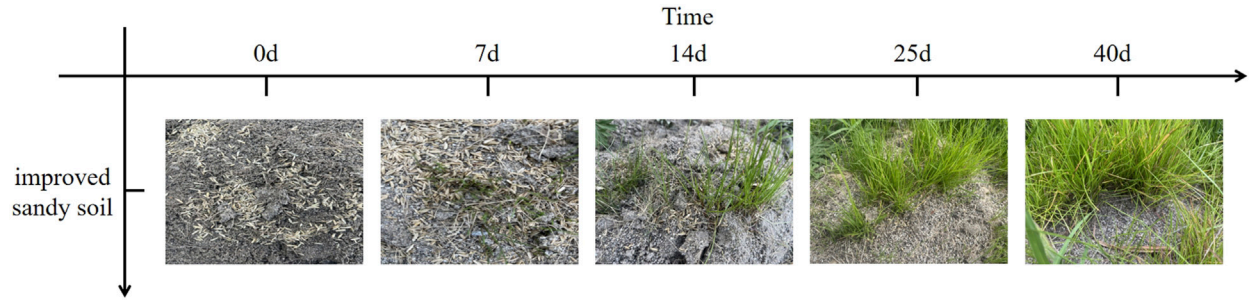

FIGURE 13
Outdoor planting in modified sandy soil.

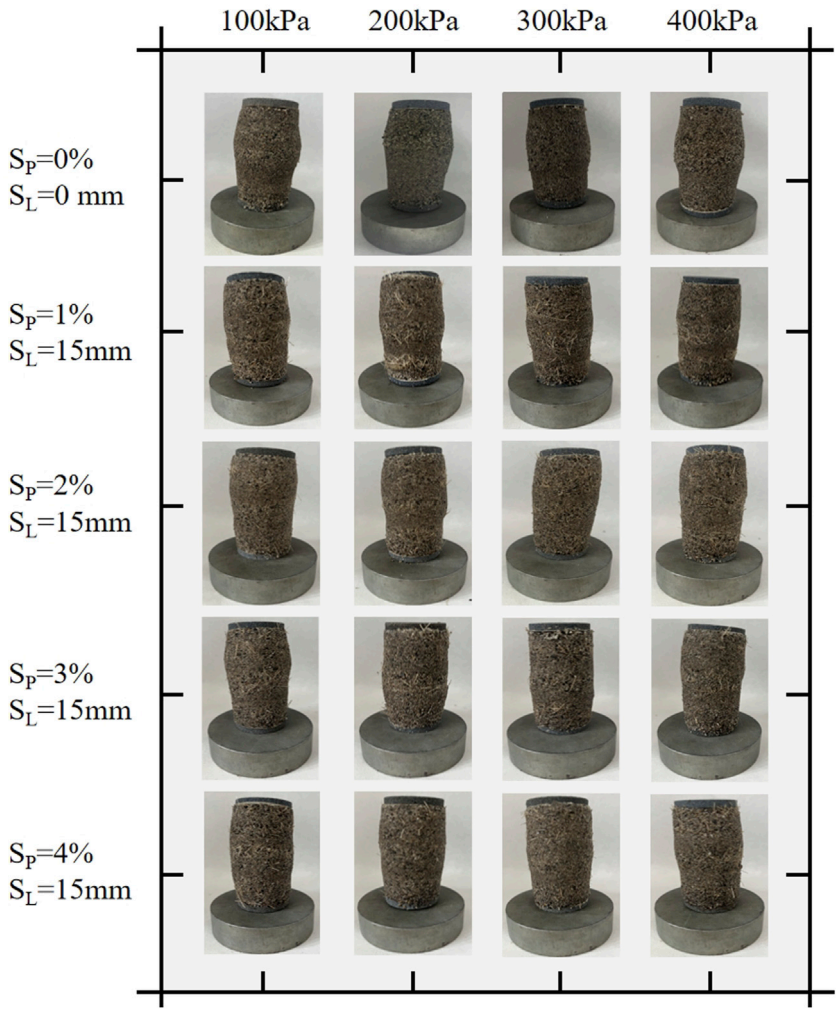

FIGURE 14
Specimen drawing after triaxial shear.

4.2 Discussion

Before conducting the experiments, outdoor seeding was performed on the PVA solution and the SF-reinforced loose accumulated sandy soil to ensure the adaptability of the materials to the high-altitude environment without harming the surrounding ecology. This seeding, performed in May during a period of ample rainfall and sufficient sunlight, resulted in the growth of native plants in reinforced sandy soil. The successful growth of these plants indicated that the modified materials were environmentally benign,

rendering them suitable for improving and reinforcing the loose slopes in the southeastern Xizang Region (Figure 13).

Ma K et al. [34] explored the potential of using polyurethane organic polymer and sisal fiber to improve the mechanical performance of sand. The results indicated a significant increase in the UCS and DTS of the reinforced sand with increasing polymer content, fiber content, and dry density. This study utilized a composite of PVA and SFs to effectively enhance the properties of loose accumulated sandy soils. Notably, when SFs with a length of S_L = 15 mm were combined with various PVA solution concentrations, the cohesion exhibited stable fluctuations, with the peak shear strength occurring at the PVA concentrations of S_P = 2% and S_P = 3%. Examination of the shear behavior of the untreated sandy soil and the modified sandy soil with 15 mm SFs at different PVA concentrations revealed that the failure mode of the samples was dominant, with no shear failure planes identified. Compared with the untreated sandy soil, the modified sandy soil exhibited a significantly reduced failure mode. At a confining pressure of 400 kPa, visible deformation was observed in the modified samples, indicating that the uneven dispersion of SFs during preparation caused aggregation and shear deformation under high confining pressures. Nevertheless, the samples with S_L = 15 mm (S_P = 3%) exhibited an improved overall stability and less noticeable compressive deformation at different confining pressures (Figure 14).

In practical engineering applications, both cost-effectiveness and safety stability are crucial. The multiphase and variable nature of geological materials can contribute to their inherent uncertainty, which is why geotechnical engineering lacks the rigor of other disciplines. As a highly practical field that operates on a conceptual design framework, geotechnical engineering relies on robust theories, reasonable experiments, and validation through practical experience as the essential foundations for successful applications.

5 Conclusion

Based on the principles of "ecological priority and green development," this study focused on modifying the loose accumulated sandy soil in southeastern Xizang using a composite of PVA solution and SFs. Various consolidated drained triaxial compression tests were performed under different confining pressures to examine the effects of varying PVA solution concentrations and SFs lengths on the strength characteristics of the modified sandy soil. SEM was employed to analyze the internal structures of the samples after shear testing. The experimental results led to the following conclusions.

(1) The stress-strain curves of the modified loose accumulated sandy soil, under varying PVA solution concentrations and SFs lengths, exhibited strain-softening behavior, characterized by a distinct peak in the deviator stress. The stress-strain relationship demonstrated elastic-plastic characteristics. The failure of the samples occurred in two main stages. At strains less than or equal to 3%, the samples were in the elastic deformation stage with a linear increase in the deviator stress. As the strain exceeded 3%, the deformation became plastic, and the deviator stress-strain relationship exhibited a nonlinear increase, with the rate of deviator stress growth gradually decreasing and trending towards a smooth decline.

(2) The incorporation of PVA solution and SFs significantly affected the peak deviator stress of the samples. As the concentration of the PVA solution and length of the SFs increased, the peak deviator stress also increased under a constant confining pressure. The relationship curve between $(\sigma_1-\sigma_3)_{max}$~$\sigma_3$ for both the untreated loose accumulated sandy soil and the modified sandy soil with the PVA solution and SFs approximated a linear trend.

(3) SEM analysis revealed that the pores between the sand particles were filled with SFs and PVA solution. The interwoven SFs bonded effectively within the adhesive formed by the PVA solution, thereby increasing the cohesion between the particles. The improved toughness of the fibers enabled them to connect both sides of the fracture surface, similar to "spider silk," providing the tensile strength that mitigated the soil deformation. Additionally, the water-soluble PVA exhibited strong adhesion to both fibers and soil particles. The hydroxyl groups in the PVA molecules bonded with the surfaces of the soil particles and fibers, enhancing the interfacial properties and improving the connection between the SFs and soil particles, which increased the overall structural stability.

(4) This study analyzed the loose accumulated sandy soil in southeastern Xizang and discovered that composite modification using a PVA solution and SFs was highly effective. The optimal combination for practical engineering reinforcement was a PVA solution concentration of S_P = 3% and SFs length of S_L = 15 mm. The modified soil exhibited a significant increase in the cohesion, rising from 24.54 kPa in the untreated sandy soil to 196.03 kPa, thus achieving both economic and reinforcement effectiveness.

Data availability statement

The original contributions presented in the study are included in the article/supplementary material, further inquiries can be directed to the corresponding author.

Author contributions

DS: Conceptualization, Data curation, Methodology, Validation, Writing–original draft, Writing–review and editing. PW: Conceptualization, Funding acquisition, Supervision, Writing–review and editing. LC: Conceptualization, Formal Analysis, Funding acquisition, Resources, Supervision, Visualization, Writing–review and editing. WZ: Conceptualization, Methodology, Supervision, Validation, Writing–review and editing. ZL: Conceptualization, Data curation, Writing–review and editing. QW: Conceptualization, Data curation, Investigation, Visualization, Writing–review and editing.

Funding

The author(s) declare that financial support was received for the research, authorship, and/or publication of this article. Key Program of Natural Foundation of Science and Technology Department of Xizang Autonomous Region, China (XZ202201ZR0068G); National Natural Science Foundation of China - Regional Innovation and Development Joint Fund Key Program (U22A20594); Key Program of Natural Foundation of Science and Technology Department of Xizang Autonomous Region, China (XZ202301ZR0033G); Sponsored by the Graduate Education Innovation Program of Xizang Agricultural and Animal Husbandry College (YJS2024-45).

Acknowledgments

We gratefully acknowledge financial support from the National Natural Science Foundation of China - We also extend our heartfelt thanks to the two participants who willingly participated in the on-site experiment and to the experts who generously shared their insights during the online survey. Additionally, we thank Wang Jiahui from Hohai University and Li Zhongyao from Chongqing Jiaotong University for their valuable insights and encouragement, which contributed to my development as a researcher.

Conflict of interest

The authors declare that the research was conducted with no commercial or financial relationships that could be perceived as potential conflicts of interest.

Publisher's note

References

1. Wang LW, Liu J, Xi LZ, Wu LL, Zheng C, Qi CQ, et al. Study on triaxial shear test of improved sandy soil based on polymer composite materials. *Hydrogeology Eng Geology* (2020) 47(04):149–157. doi:10.16030/j.cnki.issn.1000-3665.201911005

2. Yuan Y, Wang C, Liang FY. Erosion characterization of sandy soil particles based on improved SSRT test method. *Chin J Geotechnical Eng* (2020) 42(S1):198–202. doi:10.11779/CJGE2020S1039

3. Wu Z, Liu J, He Y, Wei JH, Song ZZ, Sun R, et al. Polymer curing agent vegetation composite improvement of sand erosion resistance characteristics. *Progr. Water Conser. Hydropower. Techno* (2021) 41(05):28–33+70. doi:10.3880/j.issn.1006.7647.2021.05.005

4. Yang F, Li ML, Wang X, Wu E, Wang F, Lv J, et al. Physical modeling test of rainfall on loess fill slopes based on NbS structure[J/OL]. *Adv Eng Sci* (2021)(05):24–34. doi:10.15961/j.jsuese.202300560

5. He J, Huang A, Ji J, Qu S, Hang L. Enzyme induced carbonate precipitation with fibers for the improvement of clay soil slopes against rainfall and surface runoff erosions. *Transportation Geotechnics* (2023) 42:101074. doi:10.1016/j.trgeo.2023.101074

6. Wang G, Sassa K. Study on the excess pore pressure generation at failure and the resulting movement of sandy slope in flume test by rainfall. *Landslides* (2000) 37(2):40–7. doi:10.3313/jls1964.37.2_40

7. Wang TL, Liu JK, Tian YG. Study on static properties of cement and lime-amended soil under freeze-thaw. *Rock Soil Mech* (2011) 32(01):193–8. doi:10.16285/j.rsm.2011.01.010

8. Wang L, Zhang K, Chen Y, Wang S, Tian D, Li X, et al. Progressive deformation mechanism of colluvial landslides induced by rainfall: insights from long-term field monitoring and numerical study. *Landslides* (2024) 1–18. doi:10.1007/s10346-024-02344-3

9. Jia K, Bingcheng W, Zhiqiu G, Zhou S, Chen H, Shen H. Research on machine learning forecasting and early warning model for rainfall-induced landslides in Yunnan province. *Scientific Rep* (2024) 14(1):14049. doi:10.1038/S41598-024-64679-0

10. Peng T, Chen N, Hu G, Tian S, Ni H, Huang L. New rulers for estimating the magnitude of catastrophic debris flows. *Nat Hazards* (2024) 1–14. doi:10.1007/S11069-024-06795-8

11. Wang S, Xue Q, Zhu Y, Li G, Wu Z, Zhao K. Experimental study on material ratio and strength performance of geopolymer-improved soil. *Construction Building Mater* (2020) 267:120469. doi:10.1016/j.conbuildmat.2020.120469

12. Williams KA, Ruiz SA, Petroselli C, Walker N, Fletcher DM, Pileio G, et al. Physical characterisation of chia mucilage polymeric gel and its implications on rhizosphere science - integrating imaging, MRI, and modelling to gain insights into plant and microbial amended soils. *Soil Biol Biochem* (2021) 162. doi:10.1016/J.SOILBIO.2021.108404

13. Bai Y, Liu J, Song Z, Chen Z, Jiang C, Lan X, et al. Unconfined compressive properties of composite sand stabilized with organic polymers and natural fibers. *Polymers* (2019) 11(10):1576. doi:10.3390/polym11101576

14. Ren F, Ding H, Dong B, Qian X, Liu J, Tan J. Study on the improvement of soil properties using hydrophilic-hydrophobic biopolymer crosslinking. *Construction Building Mater* (2024) 415:415135101. doi:10.1016/J.CONBUILDMAT.2024.135101

15. Zhang JR, Liu JH, Cheng Y, Jiang T, Sun D, Saberian M, et al. Water-retention behaviour and microscopic analysis of two biopolymer-improved sandy soils. *Construction Building Mater* (2023) 403. doi:10.1016/J.CONBUILDMAT.2023.133202

16. Li Z, Zhao Z, Shi H, Li W, Wang B, Wang P. Experimental investigation of mechanical, permeability, and microstructural properties of PVA-improved sand under dry-wet cycling conditions. *Front Phys* (2021) 9:761754. doi:10.3389/fphy.2021.761754

17. Zhao Z, Li W, Shi H, Li Z, Li J, Zhao C, et al. Strength of coarse-grained soil stabilized by poly (vinyl alcohol) solution and silica fume under wet–dry cycles. *Polymers* (2022) 14(17):3555. doi:10.3390/polym14173555

18. Cherdsak S, Suksun H, Chakkrid Y, Arul A Evaluation of polyvinyl alcohol and high calcium fly ash based geopolymer for the improvement of soft Bangkok clay. *Transportation Geotechnics* (2021):27100476. doi:10.1016/j.trgeo.2020.100476

19. Fabian DRC, Durpekova S, Dusankova M, Hanusova D, Bergerova ED, Sedlacik M, et al. Renewable whey-based hydrogel with polysaccharides and polyvinyl alcohol as a soil amendment for sustainable agricultural application. *Int J Biol macromolecules* (2024) 259:129056. doi:10.1016/J.IJBIOMAC.2023.129056

20. Tang C, Shi B, Gao W, Chen F, Cai Y. Strength and mechanical behavior of short polypropylene fiber reinforced and cement stabilized clayey soil. *Geotextiles and Geomembranes* (2006) 25(3):194–202. doi:10.1016/j.geotexmem.2006.11.002

21. Oliveira VJP, Correia SAA, Teles CPNMJ, Custódio GD. Effect of fibre type on the compressive and tensile strength of a soft soil chemically stabilised. *Geosynthetics Int* (2016) 23(3):171–82. doi:10.1680/jgein.15.00040

22. Memon A, Nakai A. Fabrication and mechanical properties of jute spun yarn/PLA unidirection composite by compression molding. *Energy Proced* (2013) 34:34830–8. doi:10.1016/j.egypro.2013.06.819

23. Marandi S, Bagheripour MH, Rahgozar R, Zare H. Strength and ductility of randomly distributed palm fibers reinforced silty-sand soils. *Am J Appl Sci* (2008) 5(3):209–20. doi:10.3844/ajassp.2008.209.220

24. Sudhakaran PS, Sharma KA, Kolathayar S. Soil stabilization using bottom ash and areca fiber: experimental investigations and reliability analysis. *J Mater Civil Eng* (2018) 30(8). doi:10.1061/(asce)mt.1943-5533.0002326

25. Almajed AA. *Enzyme induced carbonate precipitation (EICP) for soil improvement* (doctoral dissertation). Arizona State University, Tempe, AZ, United States (2017).

26. Huang Z. *Preparation and properties of the sword-hemp fiber-enhanced polymer-based composites [D]*. Jinan: University of (2017).

27. Patil S, Bhaskar R, Xavier RJ. Optimization of rheological and mechanical properties of sustainable lateritic self-compacting concrete containing sisal fiber using response surface methodology. *J Building Eng* (2024) 84:84108574. doi:10.1016/J.JOBE.2024.108574

28. Song H, Liu T, Gauvin F, Brouwers H. Investigation of sisal fiber incorporation on engineering properties and sustainability of lightweight aggregates produced from municipal solid waste incinerated bottom ash. *Construction Building Mater* (2024) 413:413134943. doi:10.1016/J.CONBUILDMAT.2024.134943

29. Zhang A, Liu K, Li J, Song R, Guo T, et al. Static and dynamic tensile properties of ultra-high performance concrete (UHPC) reinforced with hybrid sisal fibers. *Construction Building Mater* (2024) 411:134492. doi:10.1016/J.CONBUILDMAT.2023.134492

30. Ekkachai Y, Pongsak W, Amorn P. A use of natural sisal and jute fiber composites for seismic retrofitting of nonductile rectangular reinforced concrete columns. *J Building Eng* (2022) 52:104521. doi:10.1016/J.JOBE.2022.104521

31. Lima RP, Barros AJ, Roque BA, Fontes CM, Lima JM. Short sisal fiber reinforced recycled concrete block for one-way precast concrete slabs. *Construction Building Mater* (2018) 187:187620–34. doi:10.1016/j.conbuildmat.2018.07.184

32. GB/T 50123-2019,Standard for geotechnical testing method[S].

33. Wu XF, Luo ZX, Chen HY. Production and application of sisal fiber. *China Fiber Inspection* (2010)(03) 59–61. doi:10.14162/j.cnki.11-4772/t.2010.03.005

34. Ma K, Liu J, Jiang CY, Ma XF, Huang LH, He CZ, et al. Experimental study on the strength of sand improved by polyurethane curing agent and sisal fiber. *J Cent South Univ* (2022) 29(02):528–545. doi:10.1007/s11771-022-4909-9